DYNAMIC DEFORMATION CHARACTERISTICS OF SOILS DETERMINED BY LABORATORY TESTS

Koichiro YOKOTA, Tsuneo IMAI and Masashi KONNO

Abstract

This is a report on research the authors have carried out on the dependency of certain dynamic deformation characteristics of soil, shear modulus G and damping constant h on shear strain γ. Our ultimate objective was to find a simple method for accurately determining G and h for any given value of shear strain γ.

The research employed laboratory dynamic soil testing of undisturbed samples of alluvial and diluvial soils. The data thus obtained was first analyzed by arranging it in graphs representing different soil types to find overall tendencies. This analysis showed considerable differences in dynamic deformation characteristics between sandy and clayey alluvial and diluvial soils.

Next, the relationships between G, h and γ were expressed as a simplified experimental formula. This formula determines G/G_0 (G_0 indicates the value of G when γ is 10^{-6}) and h in relationship to two experimental constants α and β, and γ. As such, it is an extremely simple formula. α and β are quantities depending on confining pressure for each soil type.

The procedure proposed by the authors in this paper may be used to determine G and h for any given soil type, N value, σ'_m (confining pressure), and γ value.

1 INTRODUCTION

Throughout a history of Japan, there have been many destructive earthquakes. Scientific knowledge relating to earthquakes now spans many areas from techniques for analyzing earthquake phenomena to aseismic design. One important aspect of earthquake technology is the analysis of ground behavior during earthquakes, which provides fundamental data for use in the aseismic design of structures.

At present, strong motion accelographs for the monitoring of ground behavior during earthquakes are in use in a number of locations throughout Japan. Methods for the forecasting of ground behavior during earthquakes as well have shown considerable advances in recent years. Ground response analysis techniques include the finite element method, wave propagation theory and the lumped mass method. The most important point in the carrying out of response analysis is the problem of working out a model for the relationship between stress and strain. Unlike metalic substances, soil possesses non-linear properties. The nature of soil must be considered in the evaluation of this stress-strain relationship. The most common method for establishing this relationship is to substitute the non-linear stress-strain relationship into an equivalent linear model. In this model, shear modulus G and damping constant h vary greatly with changes in strain level. This phenomenon is referred to as "strain dependence".

Changes in soil dynamic deformation characteristics (i.e., shear modulus G and damping constant h) with changes in strain vary greatly according to soil type and ground conditions (confining pressure, stress history, etc.).

If these varying conditions can be well understood and the values of G and h for the given soil type and ground conditions can be found, this would constitute a major contribution to the forecasting of ground behavior during earthquakes for use in earthquake engineering.

This is the ultimate objective of this paper. The dynamic deformation characteristics of soil are investigated using data from laboratory tests of undisturbed soil samples and a considerable amount of other data. On the basis of our findings we present a proposal for a practical method of expressing the relationships between G, h and γ.

2 EQUIPMENT AND METHODS USED

2-1 Principles of Measurement

2-1-1 Resonant Column Soil Test

The resonant column soil test determines shear modulus G of samples. In this test, usually the bottom of the soil specimen is fixed and torsion and rotational excitation force are applied at the top of the specimen. Resonant frequency of the movable portion is measured and from this G is calculated. Figure 1 shows the principle of this test. In the figure,

M=input power
J_t=rotational inertia of the top mass
J_s=rotational inertia of the specimen
ρ_s=density of the specimen
G_s=shear modulus of the specimen

The following formula expresses equation of moment when excitation is applied to the specimen.

$$\rho \frac{\partial^2\theta}{\partial t^2} = G \frac{\partial^2\theta}{\partial x^2} \tag{1}$$

where t=time
θ=torsional angle
x=distance from end of the specimen

Boundary conditions are as follows:
(bottom end)

$$\theta \equiv 0 \qquad \text{at} \quad x=0 \tag{2}$$

(top end)

$$M_0 e^{i\omega t} - J_A \frac{\partial^2\theta}{\partial t^2} - K_\theta - \int_0^R \tau \cdot 2\pi r^2 \cdot dr = 0 \qquad \text{at} \quad x=L \tag{3}$$

where J_A=rotational inertia of upper mass
K_θ=spring constant
τ=shear stress on upper surface of the specimen
R=radius of sample

J_A and K_θ may be determined by calibration of the testing apparatus.

When solving formula (1) for the above conditions, if we specify that the specimen is in a reasonant state, G may be expressed as follows:

$$G = \rho\left(\frac{2\pi f_n L}{F}\right) \tag{4}$$

$$F \tan F = \frac{J_s}{J_A - \dfrac{K_s}{(2\pi f_n)^2}} \tag{5}$$

where f_n=resonant frequency
J_s=rotational inertia of the specimen

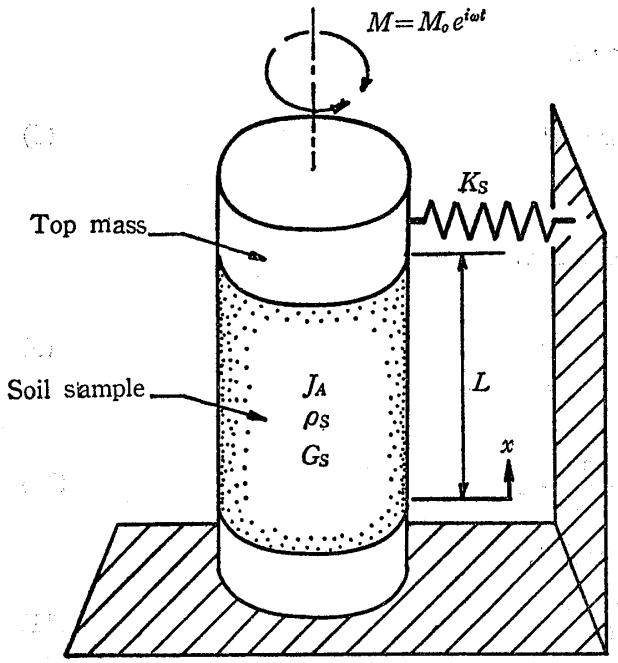

Fig. 1 Principle of the resonant column test

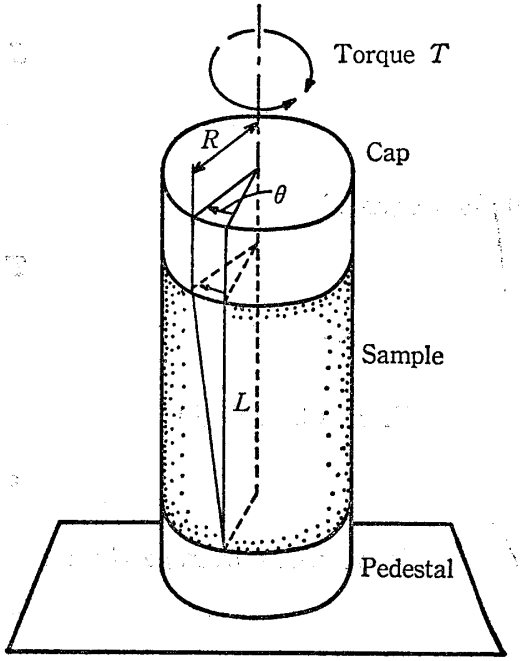

Fig. 2 Principle of the cyclic torsional test

Also, shear strain γ which corresponds to the measured value of G may be determined by using velocity amplitude which is measured near the top of the specimen. If we specify a as the distance from the center of the specimen to the velocity sensor, velocity as V, resonant frequency as f_n, radius of the specimen as R, length of the specimen as L and the value for equivalent strain as that strain at a point 2/3 of the distance from the center to the circumference of the specimen, we get the following formula:

$$\gamma=\frac{R}{2\pi f_n}\times\frac{R}{a}\times\frac{2}{3}\times\frac{1}{L}$$

$$=\frac{R^2}{3\pi a\cdot f_n\cdot L} \tag{6}$$

Consequently, of all the values measured during testing, the most important are f_n and V. In addition, damping constant h is often measured with resonant column soil testing apparatus, but this value is not measured in the present study.

2-1-2 Cyclic Torsional Apparatus

Generally, in this test the bottom end of the specimen is fixed and torsion is repeatedly applied to the top. By knowing the amount of torque T and the rotational angle θ, G, h and γ are determined. This principle is illustrated in Figure 2. The device used in the present study was of this type. It delivered a sinusoidal excitation force of 0. 1 to 3 Hz (input of a random wave from an external source was also possible). Below are the methods for determining G, h and γ from measured torque and rotational angle.

Shear force is expressed according to the following formula:

$$S=\int_0^R \tau\cdot 2\pi r\cdot dr \tag{7}$$

Here, if we assume that τ increases proportionately in the direction of the radius, $\tau=k\cdot r$ and

$$S = 2\pi k \int_0^R r^2 \cdot dr$$

$$= \frac{2\pi}{3} \cdot k \cdot R^3 \tag{8}$$

and for torque T

$$T = \int_0^R \tau \cdot 2\pi r^2 \cdot dr$$

$$= \frac{2\pi}{4} \cdot k \cdot R^4 \tag{9}$$

From (8) and (9)

$$S = \frac{4}{3} \cdot \frac{1}{R} \cdot T \tag{10}$$

If we define average shear stress $\bar{\tau}$ as $\bar{\tau} = S/A$,

$$\overline{\tau} = \frac{4T}{3\pi R^3} \tag{11}$$

Now, if we adopt 2/3 of maximum strain at the outer circumference as is customarily done, average shear strain $\bar{\gamma}$ corresponding to G becomes

$$\overline{\gamma} = \frac{R \cdot \theta}{L} \cdot \frac{2}{3} \tag{12}$$

As shown in Figure 3, damping constant h is determined from the hysterisis loop.

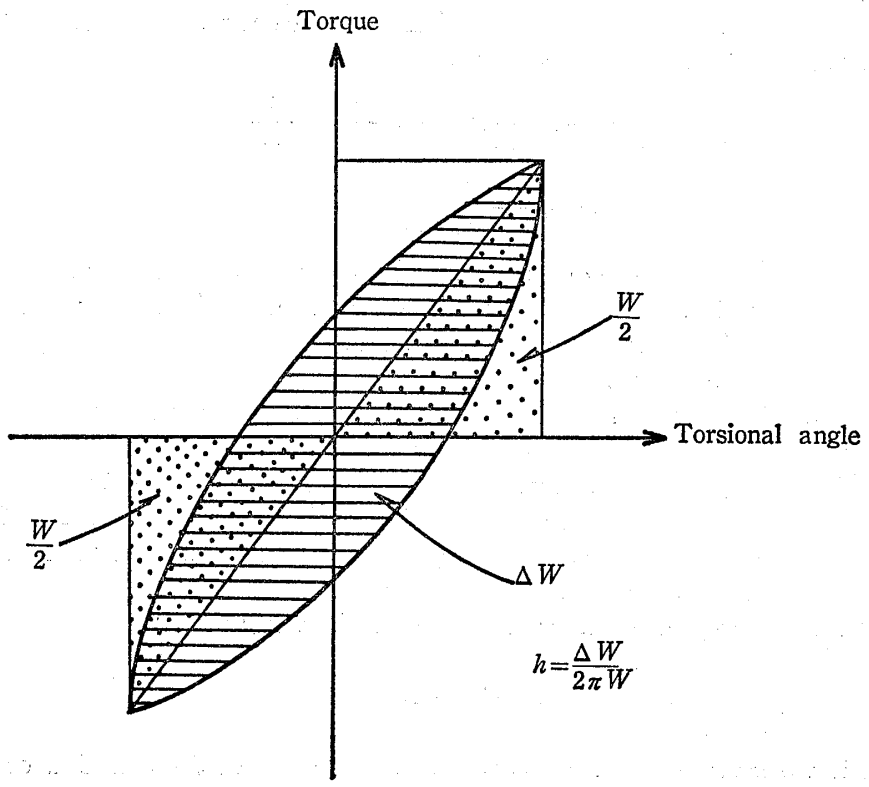

Fig. 3 Definition of damping constant h

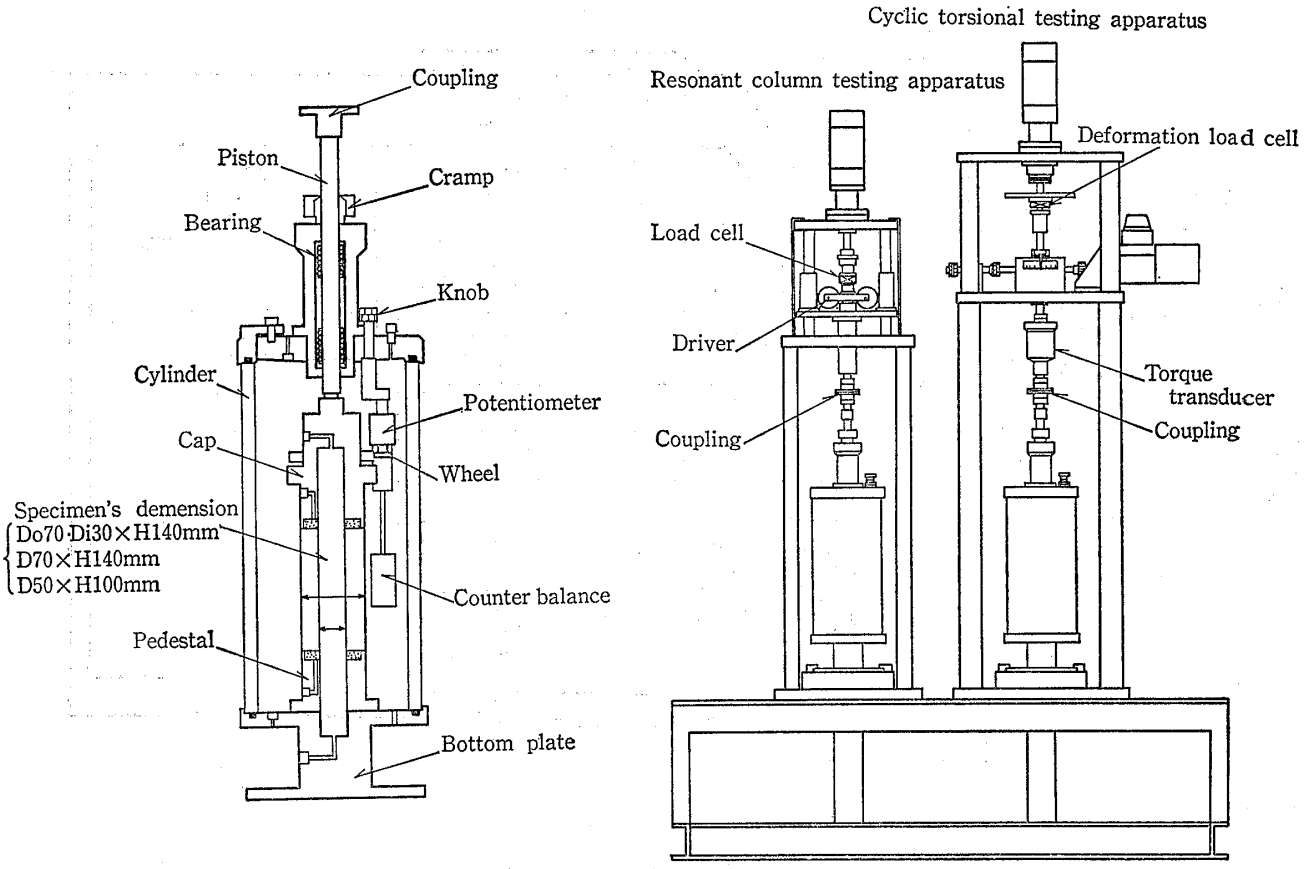

Fig. 4 Testing apparatus

2-2 Testing Apparatus

Figure 4 shows the testing apparatus. The testing apparatus used in the present study is a system in which the resonant column soil testing and cyclic torsional testing may be carried out in the same cell. Also, because the same loading stage is used in both tests, both testing apparatus are shown in the same figure. Figures 5(a) and 5(b) illustrate the test methods. As shown in Figure 5(a), which illustrates the method of determining resonant frequency f_n in the resonant column soil test, this is done by describing the Lissajous curve of input force and response velocity. Using this method to determine f_n makes measurement a simple process.

2-3 Samples Used in the Tests

In all, 79 samples were used in the tests (alluvial sandy soil, 19; alluvial clayey soil, 15; dilluvial sandy soil, 24 [6 of which were volcanic ash]; diluvial clayey soil, 21 [7 of which were volcanic ash]). Table 1 summarizes the types of soil tested.

2-4 Testing Methods

Both the resonant column soil test and the cyclic torsional test were carried out on all samples. The resonant column soil testing apparatus was used for testing of up to $10^{-6}>\gamma\geqq10^{-4}$ and cyclic torsional testing apparatus was used for testing of up to $10^{-4}>\gamma\geqq10^{-2}$. First, let us explain testing conditions for each test. Following this, a more detailed explanation of each testing method will be given. Table 2 lists the testing conditions in common for both tests.

2-4-1 Resonant Column Soil Test

After consolidation the samples are subjected to vibratory loading. At first, input force is kept as small as possible. (This is controlled by monitoring response velocity. Then

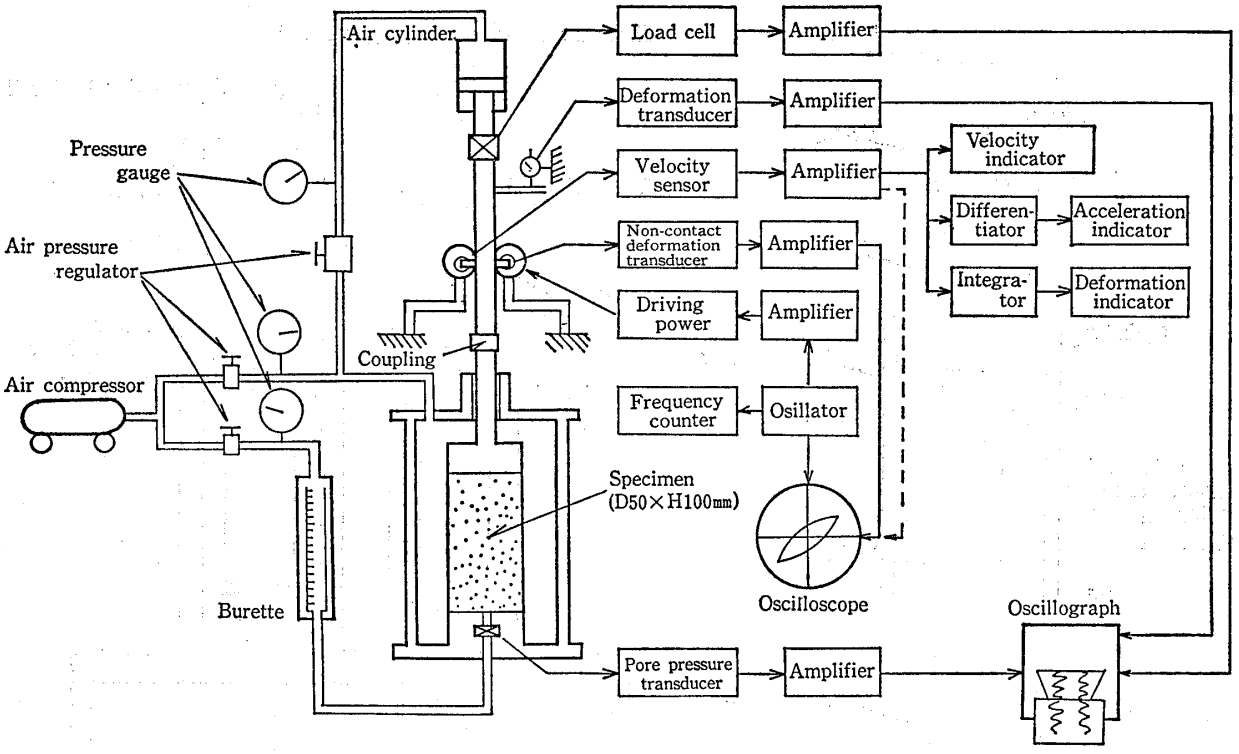

Fig. 5 (a) Schematic diagram of resonant column test

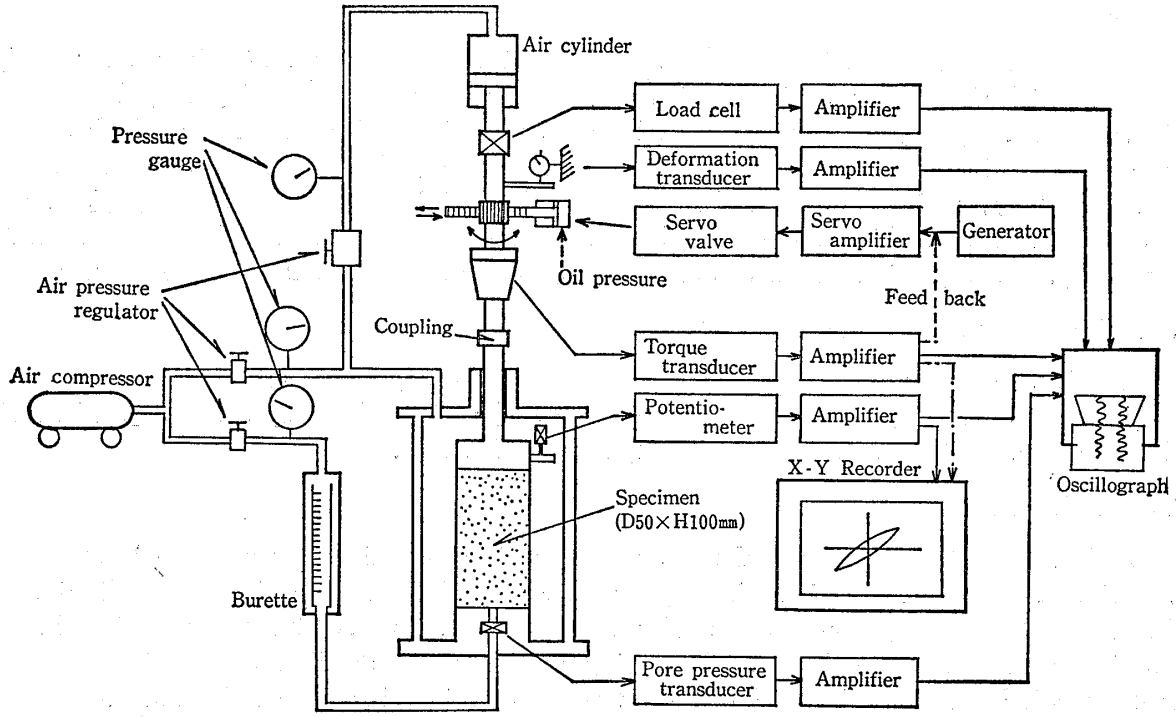

Fig. 5 (b) Schematic diagram of cyclic torsional test

Table 1 Samples used in testing

Site	Soil type	Remarks	
A (Osaka pref.)	A_s	σ'_v=0.6～0.7kg／cm²	D_{50} =0.25～0.27mm N =7～9
B (Niigata pref.)	A_s	σ'_v=0.55～1.35kg／cm²	D_{50} =0.13～0.335mm N =4～15
C (Saitama pref.)	A_s	σ'_v=0.25～0.70kg／cm²	D_{50} =0.17～0.215mm N =4～20
	A_c	σ'_v=1.2～2.6kg／cm²	ω =52.1～85.4% N =1
D (Tokyo metropolis)	A_s	σ'_v=0.20～0.25kg／cm²	D_{50} =0.24mm N =23～24
	D_s	σ'_v=1.0～2.25kg／cm²	D_{50} =0.215～0.25mm N =22～37
	D_c	σ'_v=0.46～3.8kg／cm²	ω =35.7～128% N =10～37
E (Hyogo pref.)	A_c	σ'_v=1.50kg／cm²	ω =57% N =7
	D_c	σ'_v=3.10～3.50kg／cm²	ω =21～46% N =15～17
F (Saitama pref.)	A_s	σ'_v=0.6～0.8kg／cm²	D_{50} =0.08～0.145mm N =3～15
	A_c	σ'_v=0.40～1.70kg／cm²	ω =42～89.3% N =2～3
G (Nagoya pref.)	A_s	σ'_v=0.37～0.80kg／cm²	D_{50} =0.143～0.15mm N =4～8
	A_c	σ'_v=1.20kg／cm²	ω =42.7% N =5
	D_c	σ'_v=1.80kg／cm²	ω =36.7% N =10
H (Chiba pref.)	D_s	σ'_v=0.90～7.0kg／cm²	D_{50} =0.095～0.155mm N =20～50
I (Aomori pref.)	V	σ'_v=0.1～2.0kg／cm²	ω =57～117.4% N =2～3

A_s : Alluvial sand, A_c : Alluvial clay, D_s : Diluvial sand,
D_c : Diluvial clay, V : Volcanic ash

Table 2 Test conditions common to the both tests

Dimension of the sample	50ϕ×100 or 70ϕ×140h (mm)
Consolidation pressure	Effective overburden pressure, isotropical
Duration of consolidation	3 hours for sandy soils 20hours for clayey soils
Degree of saturation	95～100%
Drain condition	Drained for sandy soils Undrained for clayey soils

resonant frequency is found.) This is done by adjusting response velocity dial while at the same time adjusting the frequency dial, taking care that strain does not increase, and looking for f_n. Determination of resonant state is done by watching the oscilloscope for when input force and response velocity waves correspond to a straight line Lissajous curve (when the two waves are out of phase by a factor of $\pi/2$). At precisely that time, read off V and f_n. Next, increase V a little (i. e., increase strain amplitude) and find f_n. Repeat this first stage measurement. Continue 6 to 8 times until γ reaches a value of about 10^{-4}. Also, measure vertical displacement, vertical load and, if necessary, pore water pressure, etc. at each stage. This 6 to 8 stage sequence constitutes one series of tests. In the present study, 3 series of tests were carried out for each specimen.

2-4-2 Cyclic Torsional Test

When the resonant column soil test is completed, next the specimen used is taken to the loading platform for conducting of the cyclic torsional test under a fixed confining pressure. When the specimen is installed on the apparatus, enough torque is applied to produce a strain in the range of 10^{-4}. At the same time, rotational angle of the specimen is also measured. The results are recorded from an electromagnetic oscillograph as a waveform and as a hysterisis loop with an XY recorder. The waveform is a sinusoidal wave with a frequency of 0.25 Hz and the number of cycles is 10 times. In all cases, records of tenth cycles are used for calculating G, h and γ. In the cyclic torsional test, these ten repetitions constitute the first stage of measurement. As γ gradually becomes larger, 6 to 8 measurements are conducted. Generally, strain at the final stage is approximately 10^{-2}.

2-5 Example of Test Results

In Figure 6 and 7, examples of test results are shown. Figure 6 shows the relationship between G and γ and Figure 7, between h and γ. While in Figure 6, there is only a small difference between the two test methods, good agreement is shown for this type of experiment.

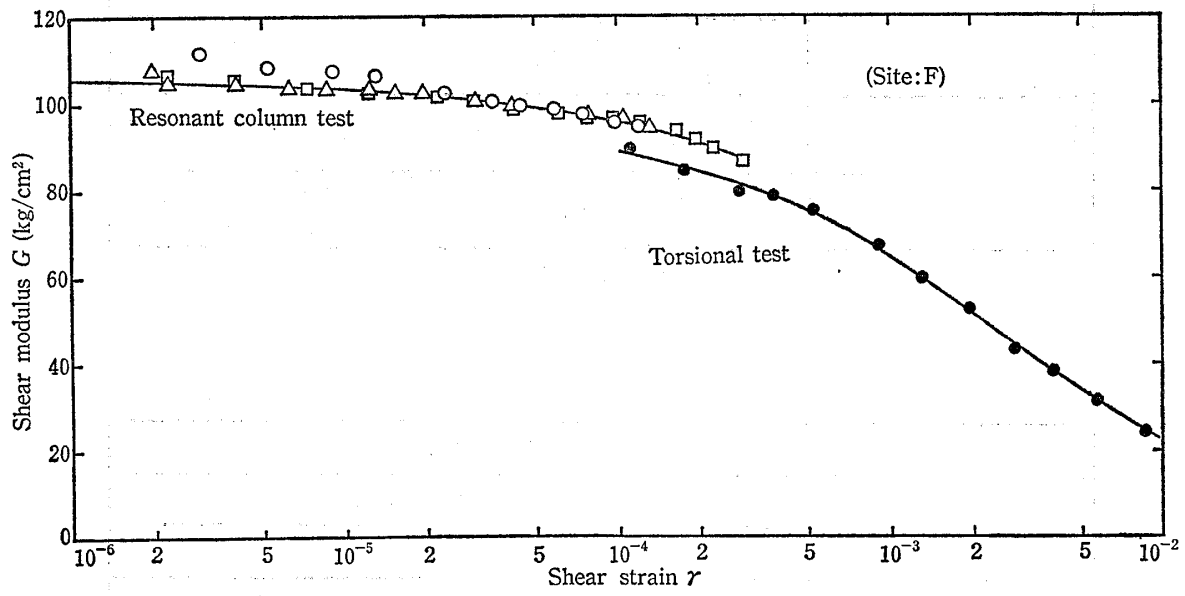

Fig. 6 Typical test results —Relationship between G and γ—

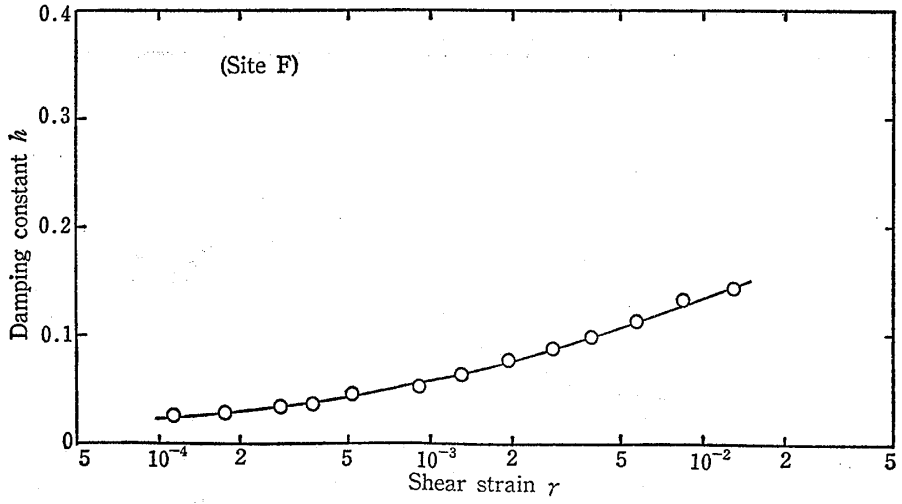

Fig. 7 Typical test results ——Relationship between h and γ——

3 DYNAMIC DEFORMATION CHARACTERISTICS OF UNDISTURBED SAMPLES ——GENERAL TENDENCIES——

Figure 8 and 9 show the overall results of our tests. In Figure 8, the Y axis represents the values obtained when G is divided by G_0 (G when $\gamma=10^{-6}$). It can be seen that in both the G/G_0 and h—γ graphs, there is a wide range of scattering of curves. Below, a more detailed explanation of overall tendencies is given for sandy and clayey soil.

3-1 Dynamic Deformation Characteristics of Sandy Soil

Figure 10 and 11 show relationships between G/G_0 and γ and h and γ in sandy soil respectively. The figures show these relationships for alluvial sandy soil and diluvial sandy soil for different ranges of effective confining pressure. From these figures, we may make the following conclusions. While A_s and D_s both extend over a wide range, the relationship between their respective greatest and least values depends on the greatest and least values of σ'_m. As for the relationship between A_s and D_s, these figures are not sufficient to decide positively.

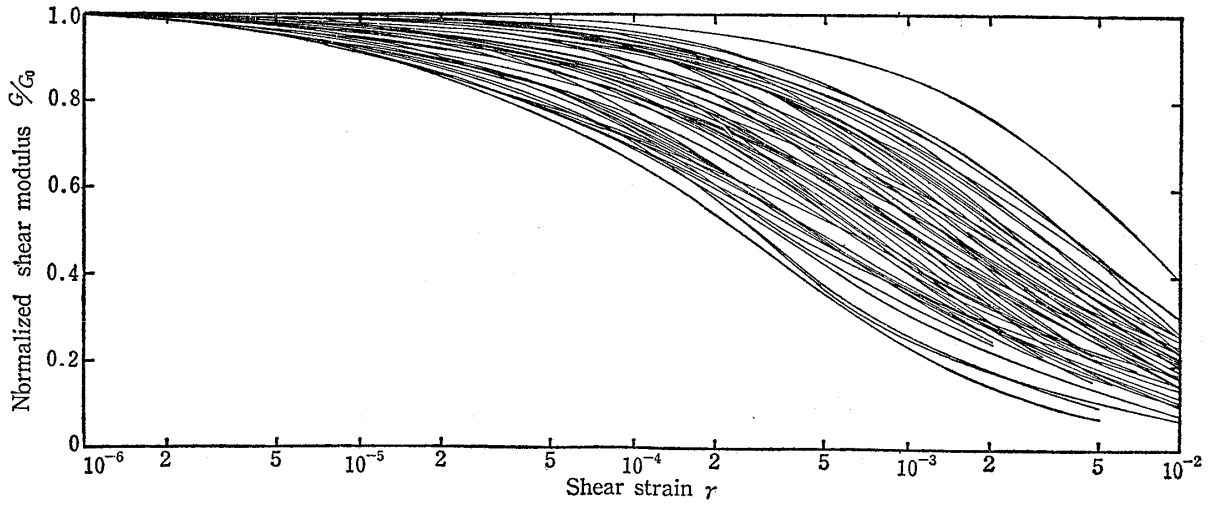

Fig. 8 Overall results of the test ——Relationship between G/G_0 and γ——

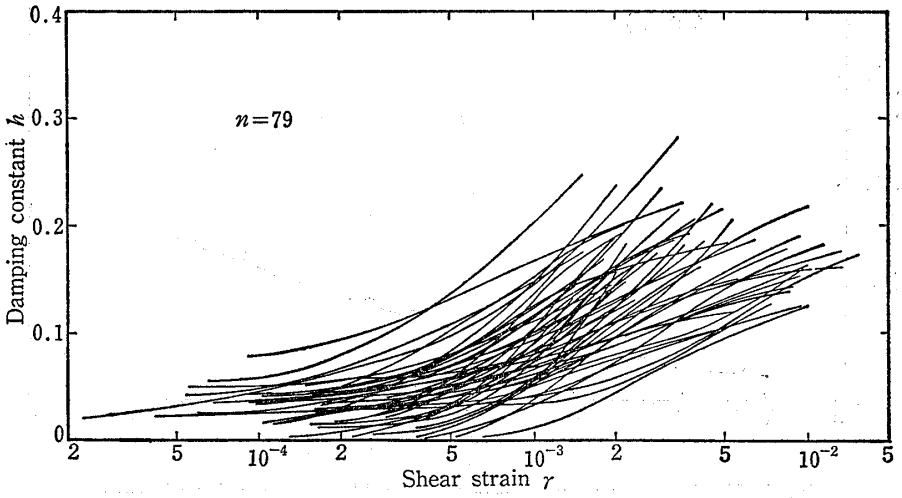

Fig. 9 Overall results of the test ——Relationship between h and γ——

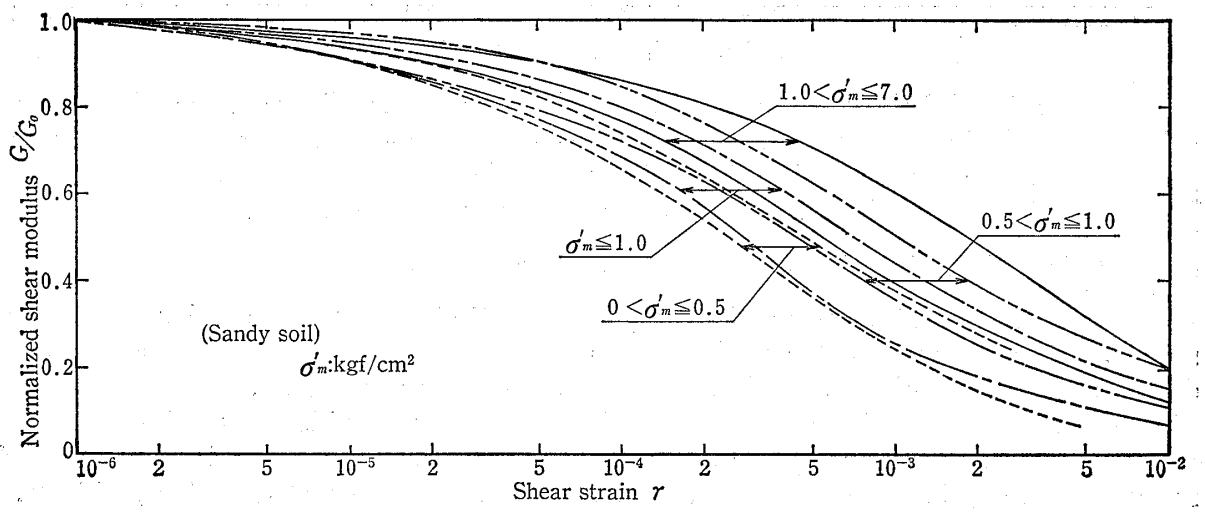

Fig. 10 G/G_0 versus γ relationship of sandy soils

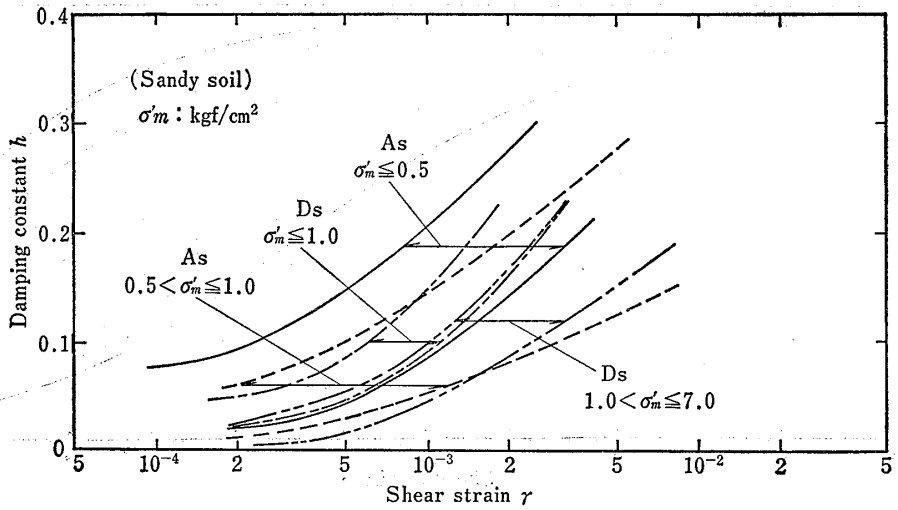

Fig. 11 h versus γ relationship of sandy soils

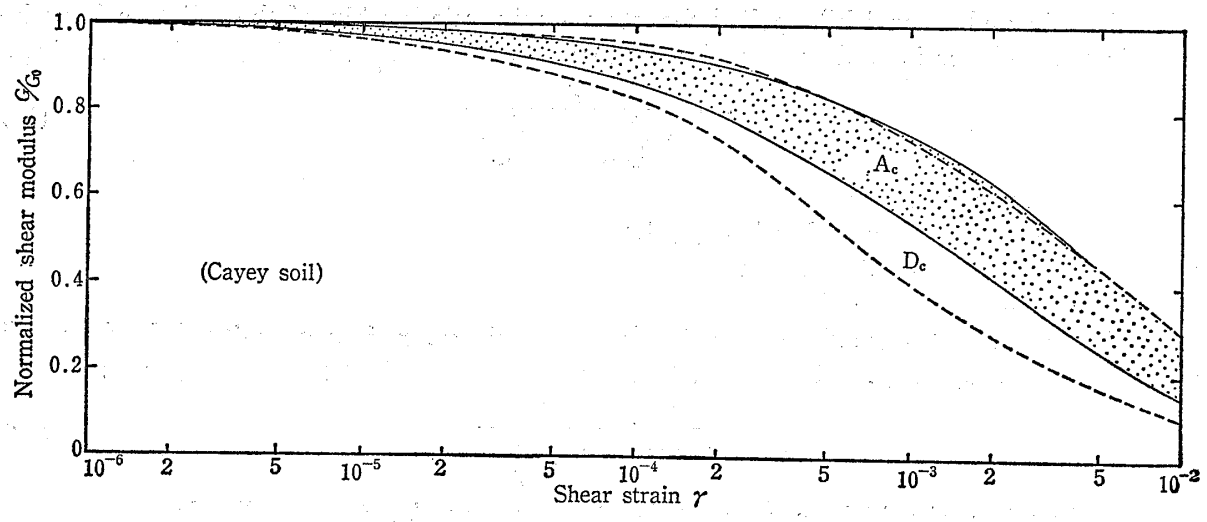

Fig. 12 G/G_0 versus γ relationship of clayey soils

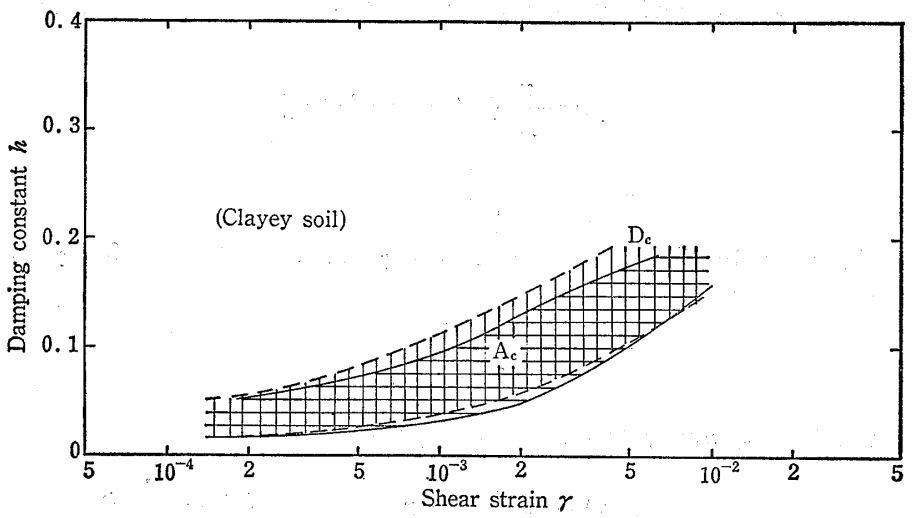

Fig. 13 h versus γ relationship of clayey soils

3-2 Dynamic Deformation Characteristics of Clayey Soil

Figures 12 and 13 show the relationships between G/G_o and γ and h and γ respectively for clayey soil. Because it may be considered that in clayey soil outstanding differences according to confining pressure would not be seen, only the ranges A_c and D_c are used. It can be seen that these ranges generally tend to overlap. If we compare with sandy soil, for the relationship G/G_o—γ, the range of values reaches a higher position on the graph for clayey soil, for the relationship h—γ, the range for clayey soil falls below that of sandy soil.

4 DISCUSSION

4-1 Proposal of Recommended Curve

As mentioned above, we have found the general tendencies for the relationships G/G_o-γ and h-γ. Below, we would like to discuss a simplified way of expressing these relationships.

Hardin and Drnevich[1] applied the stress-strain relationship of the soil to a hyperbolic model. In this case, as is well-known, shear stress τ is expressed according to the following:

$$\tau = \frac{\gamma}{\frac{1}{G_{max}} + \frac{\gamma}{\tau_{max}}} \tag{13}$$

where τ=shear stress
G_{max}=maximum G value ($\fallingdotseq G_o$)
γ=shear strain amplitude
τ_{max}=shear strength

Hardin and Drnevich[1] re-defined reference strain γ_r. γ_r is a quantity defined according to the relationship τ_{max}/G_{max}. Formula (13) may be expressed in the following way:

$$\frac{G}{G_{max}} = \frac{1}{1 + \frac{\gamma}{\gamma_r}} \tag{14}$$

Although γ_r should be a constant for the same sample, it generally does not come out to be a constant if we solve for it from Formula (14), which uses G/G_{max} and γ. We may suppose that this has to do with the difference between actual and theoretical soil behavior in Formula (13). Hardin and drnevich[1] have suggested the following formulas to account for this difference:

$$\gamma_h = \frac{\gamma}{\gamma_r}[1 + a \exp^{-b(\gamma/\gamma_r)}] \tag{15}$$

$$\frac{G}{G_{max}} = \frac{1}{1 + \gamma_h} \tag{16}$$

The authors would like to postulate this γ_r as a coefficient for γ and propose a different formula:

$$\frac{G}{G_{max}} = \frac{1}{1 + \frac{\gamma}{A(\gamma)}} \tag{17}$$

If we use G/G_{max} and γ to express $A(\gamma)$, we get

$$A(\gamma) = \frac{R}{1-R} \cdot \gamma \qquad \left(R = \frac{G}{G_{max}}\right) \tag{18}$$

Consequently, assuming as $G_{max}=G_o$ and if we calculate back from actual experimental results, it is possible to determine $A(\gamma)$. Figure 14 shows relationships between $A(\gamma)$ and γ, determined in this way. It can be seen that both values describe a straight line on the logarithmic graph paper. Here we have only shown a few examples, but they prove to be similar to other test results. Because when $R=1$ in Formula (18), $A(\gamma)$ becomes infinite, so if, for example, we plot $A(\gamma)$ against as in Figure 14, the value becomes large within a very small range of values for γ. However, if we use Formula (17) again to calculate G/G_{max}, about all we get is error that can be ignored. From the above, we find that if we express $A(\gamma)$ as

$$A(\gamma) = \frac{1}{\alpha} \cdot \gamma^{1-\beta} \tag{19}$$

G/G_o ($=G/G_{max}$) becomes

$$\frac{G}{G_o} = \frac{1}{1 + \alpha\gamma^{\beta}} \tag{20}$$

In other words, if we know α and β in Formula (20), we can determine G/G_o values for optional γ values. Thus, let us consider the possible relationships between α and different

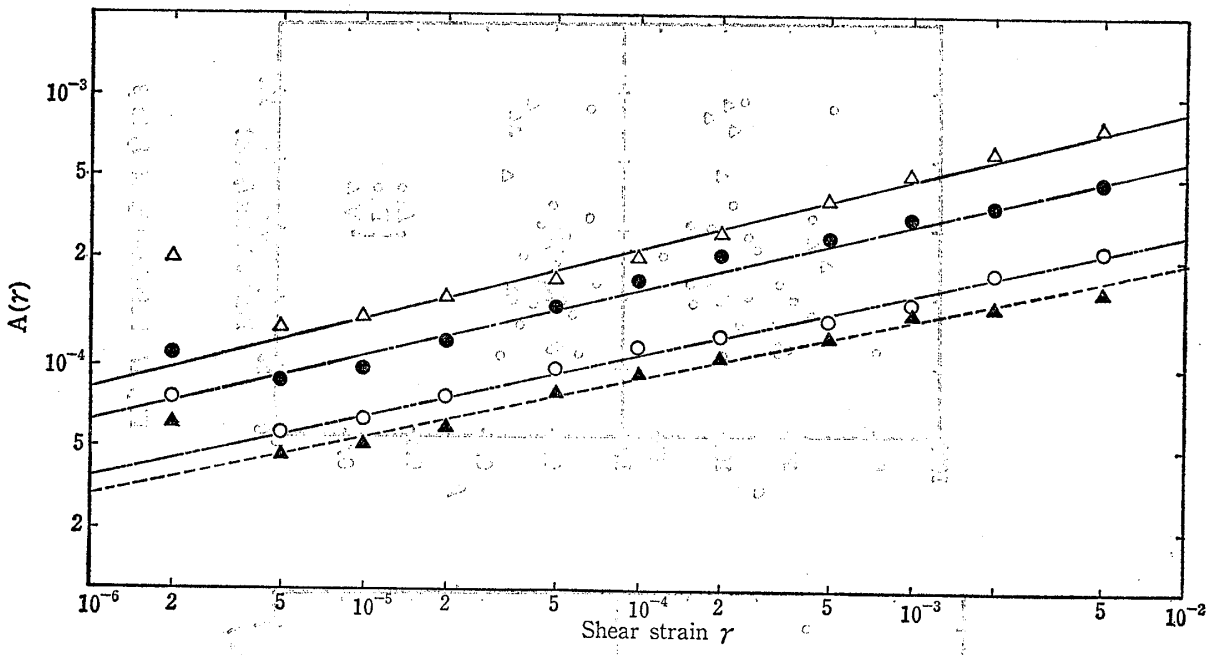

Fig. 14 Relationship between $A(\gamma)$ and γ

soil types and the same for β.

Soil may be divided into the following 4 types: alluvial sandy soil (A_s); diluvial sandy soil (D_s); alluvial clayey soil (A_c) and diluvial clayey soil (D_c). For reference, we have plotted values for volcanic ash (V) separately from diluvial soil.

While this is not necessarily the optimum system of classification for expressing dynamic deformation characteristics of soil, from a practical standpoint, it serves the purposes of the following discussion.

Figure 15 shows the relationships of σ'_m to α. We know that there is a dependency on confining pressure in the curve G/G_o—γ for sandy soil. The figure reconfirms this. Thus, as σ'_m increases, α decreases and G/G_o in Formula (8) becomes bigger. We may suppose that this relationship is to some degree present for diluvial clayey soil, but for alluvial clayey soil it appears that there is no relationship between α and σ'_m.

Figure 16 plots the values of β against σ'_m. For alluvial soil, no clear relationship can be seen. Of the diluvial soils, for sandy soil we get a curve bearing to the lower right and for clayey soil, a curve bearing to the upper right. As β values increase, G/G_o increases within the range $\gamma<1$. Consequently, if we consider the relationships from the standpoint of σ'_m—β only, for diluvial sandy soil G/G_o becomes smaller as σ'_m becomes larger, while for diluvial clayey soil G/G_o becomes larger.

Figure 17 shows α and β values for I_p values. Researchers have attempted to find relationships between I_p and dynamic deformation characteristics of clayey soil. Among this research, there is a theory that with increases in I_p, the value for G/G_o increases[2] while there is also the reverse theory that G/G_o decreases.[3] From Figure 17, we may draw the following conclusions in relation to this problem.

(1) In alluvial clayey soil, there is no clear relationship either between I_p and α or between I_p and β. Thus, there is no clear relationship between G/G_o and I_p.

(2) We find that for diluvial clayey soil, —including volcanic ash— α has a tendency to bear to the lower right (with no clear tendency for β). Thus, while I_p values are large, the G/G_o—γ curve appears to shift upwards.

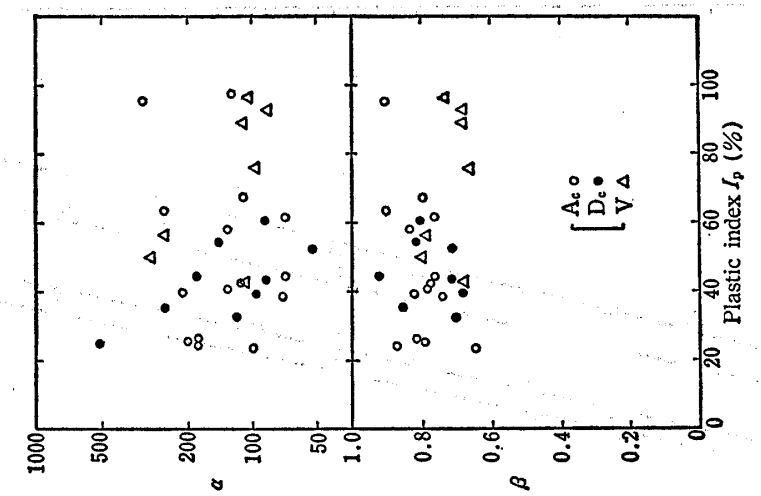

Fig. 17 Relationship of I_p to β

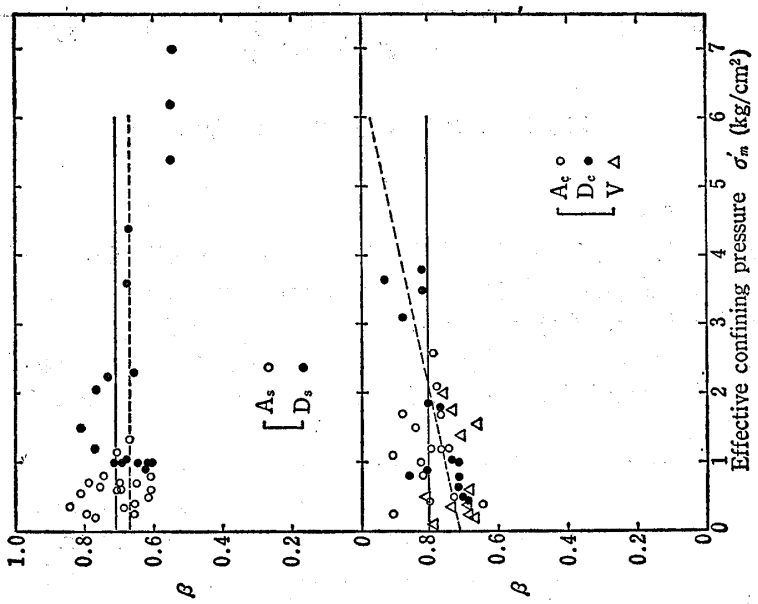

Fig. 16 Relationship of σ'_m to β

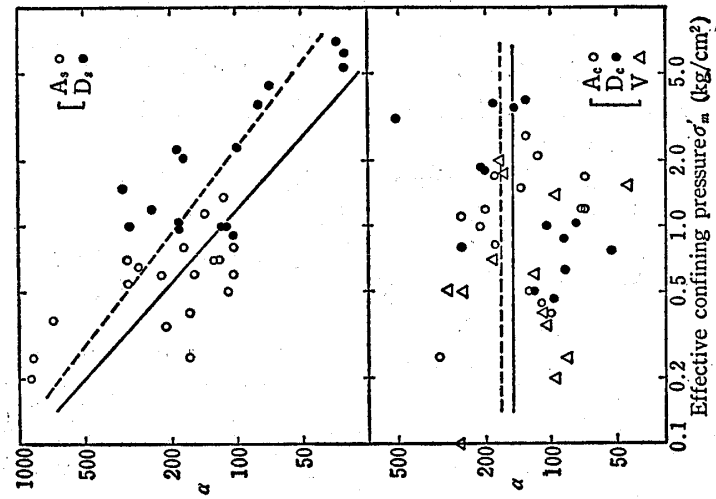

Fig. 15 Relationship of σ'_m to α

Concerning the above mentioned relationships between σ'_m and α and σ'_m and β, for those cases in which relatively good relationships were seen (for α, in A_s and D_s, for β in D_c only) experimental coefficients were determined by using the least square method. For those cases in which no clear correlations can be seen, average α and β values were taken irrespective of relationship with σ'_m. Table 3 shows these results.

Table 3 Adopted values of α and β

Soil type	α	β
A	$120\sigma'_v{}^{-0.89}$	0.71
A	150	0.80
D	$190\sigma'_v{}^{-0.77}$	0.67
D	170	$0.0425\sigma'_v+0.71$

From the above, values for α and β as functions of σ'_m and as average values for each type of soil are obtained. Thus, it is possible to calculate G/G_0 for any strain. However, it is important to note that, because of the nature of Formula (20), when $\gamma=10^{-6}$, G/G_0 is less than 1. Figure 18 shows h–G/G_0 relationships for all data. The relationship is obtained by cancelling out γ in the two relationships G/G_0–γ and h–γ. According to Hardin and Drnevich, this relationship is a straight line, but, as shown in the figure, results from experiments show the relationship to be a curve. In any case, by adopting this relationship, we find that there is a relative reduction in the scatter described by our data. If we express the average curve in the figure numerically, we get

$$\log h=-1.428\frac{G}{G_0}-0.460 \qquad (21)$$

Thus, we have found that if soil type, effective confining pressure and strain are given, we can express the overall G/G_0–γ and h–γ curves.

Figure 19 through 21 are recommended curves for each type of soil for G/G_0–γ and h–γ, obtained by using the above formula. Figure 19 is for alluvial sandy soil, Figure 20 for diluvial sandy soil and Figure 21 is for clayey soil. On the basis of Figures 19 through 21, the following statements can be made:

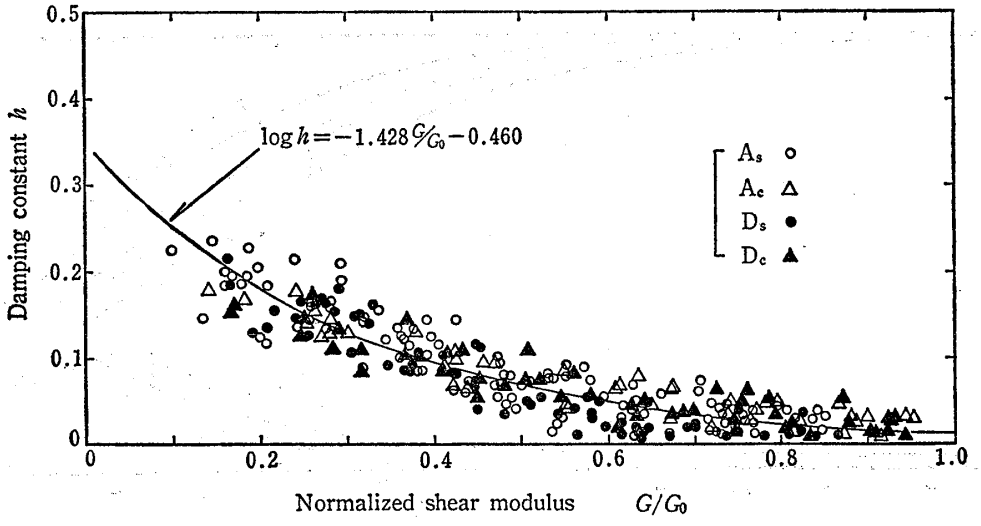

Fig. 18 Relationship between h and G/G_0

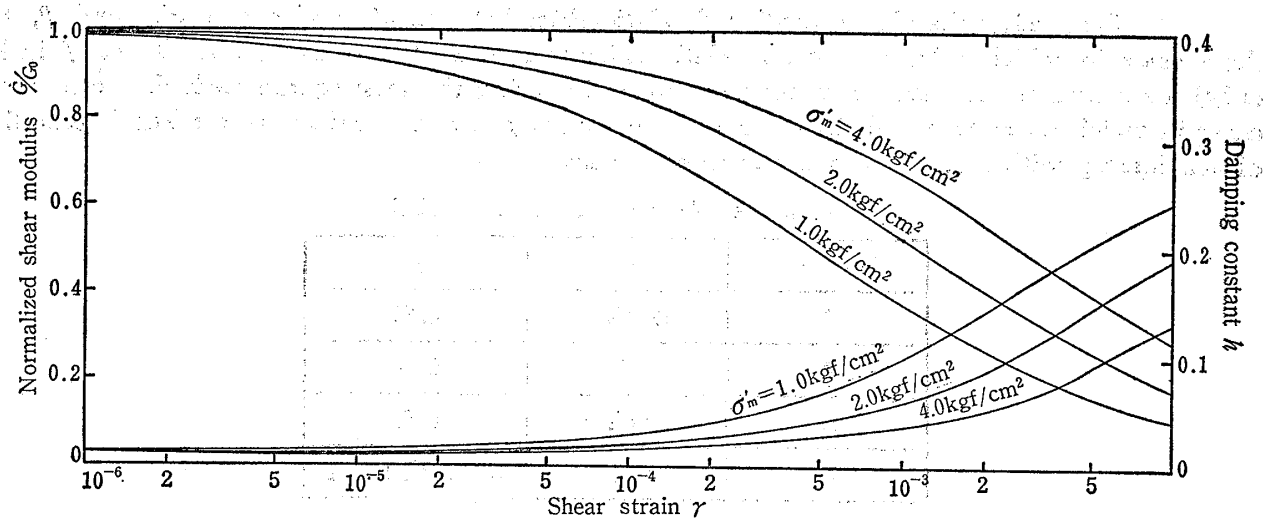

Fig. 19 Proposed curves of alluvial sand

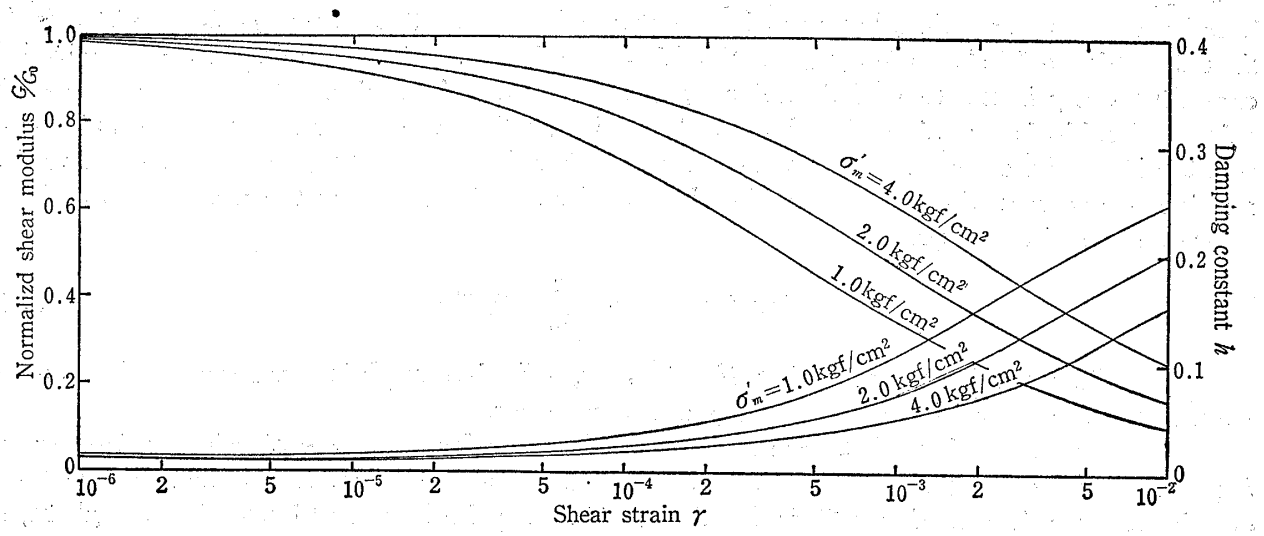

Fig. 20 Proposed curves of diluvial sand

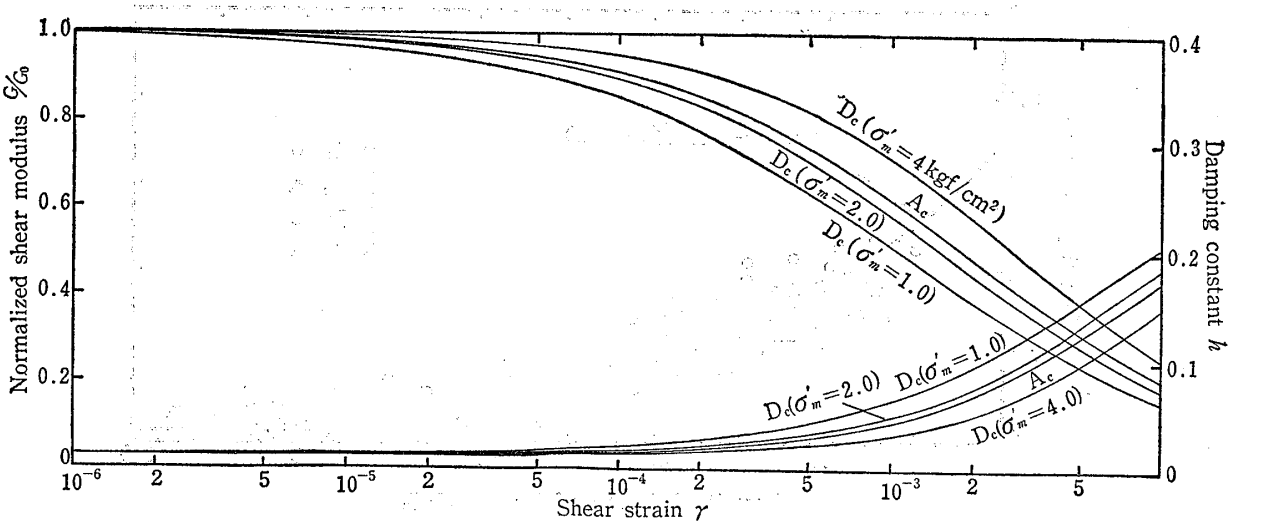

Fig. 21 Proposed curves of clayey soil

(a) Both alluvial sandy soil and diluvial sandy soil show a high degree of dependency on confining pressure.

(b) The G/G_o $-\gamma$ curve points downward under same confining pressure for diluvial soil more than for alluvial sandy soil, while the $h-\gamma$ curve points upward under same confining pressure for diluvial soil more than for alluvial sandy soil.

(c) In alluvial clayey soil, both α and β have average values. Thus, there is no change under confining pressure. However, in diluvial clayey soil, there is a dependency on confining pressure, the same as in sandy soil.

(d) In comparing alluvial clayey soil and diluvial clayey soil, depending on the range of confining pressure, the vertical relationships between $G/G_o-\gamma$ and $h-\gamma$ curves differ. Thus, in confining pressures below 2 kg/cm^2, the diluvial clayey soil $G/G_o-\gamma$ curve falls below that of alluvial clayey soil, while the $h-\gamma$ curve is above.

4-2 Comparison with Previously Proposed Curves

Figure 22 compares previously proposed curves[4),5),6),7),8)] and the authors' proposal for sandy soil. The authors descrived representative curves for standard Toyoura sand and diluvial sand using values for confining pressure under various conditions selected by the data presented by Kokusho et al.[4),5)]

Diluvial sand samples used were undisturbed samples. The $G/G_o-\gamma$ curves determined by Tatsuoka et al. were based on average values from experimental results obtained from a number of different types of disturbed sand samples. The $h-\gamma$ curves of Tatsuoka et al[6),7)]. were derived by taking average curves from their own $h-G/G_0$ curves for Iruma sand and Banno-su sand (disturbed sample tests) and the $G/G_o-\gamma$ curve in Figure 20 and cancelling out G/G_o between the two. The range indicated by Seed is based on the results of efforts by many researchers up to 1970.[8)]

Looking at Figure 22 we may make the following statements:

(a) Of the authors' proposed curves, in alluvial sandy soil, the $G/G_o-\gamma$ curve is positioned highest on the graph, while the $h-\gamma$ curve is lowest. However, on close inspection, we find that within a small range of strain, there is a good correlation with the curves taken by Kokusho for Toyoura sand. Also, this curve varies considerably from the formula proposed by Tatsuoka et al.

(b) Although there is an insufficiency of previous data on diluvial sandy soil, we see

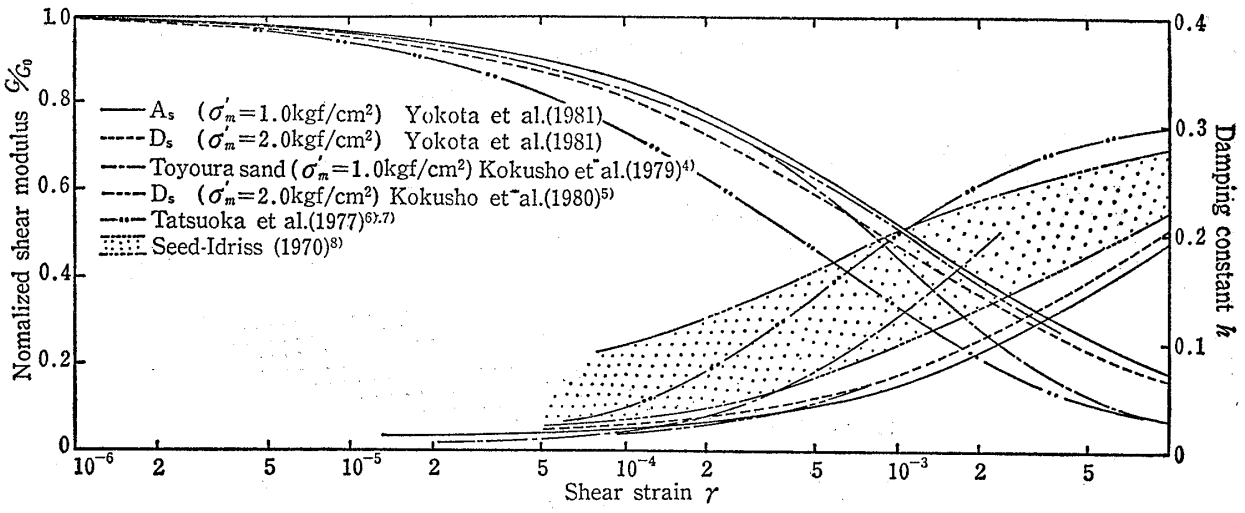

Fig. 22 Comparison with previously proposed curves of sandy soil

from the figure that there is extremely good correlation with Kokusho's undisturbed samples.

In looking over the results for diluvial sandy soil, when we consider that results obtained by the authors' equipment and equipment used by Kokusho et al., we may conclude that both researches yielded approximately the same results. Consequently, we may suppose that we may disregard differences between results due to differences in equipment between the authors' data and that of Kokusho et al. for alluvial sandy soil as well. Although there should be no difference in results due to test equipment used, practical experience tells us that differences do result.

Considering the matter from this point of view, if we compare the results obtained by Kokusho et al. with Toyoura sand and the authors' proposed curves, even though there is good correlation between the two within a small range of strain, if we look at areas of large strain, we find that both the G/G_o–γ and h–γ curves show discrepancies between the two experimental results. We may attribute this to the difference between disturbed and undisturbed sand.

Figure 23 compares previous recommended curves[8),9),10),11)] and the authors' recommended curve for clayey soil. The curve attributed to Ohsaki in the figure is an average curve calculated by the authors on the basis of Ohsaki's experimental results.

From this figure, we may draw the following conclusions:

(a) The authors' proposed G/G_o–γ curve is the highest in the graph of all the curves, while the authors' proposed h–γ is the lowest.

(b) The authors' G/G_o–γ curve is relatively close to that of Iwasaki[3),9),10)] et al., for alluvial clayey soil.

(c) The authors' results come close to the lower limit found by Seed for both alluvial and diluvial soil.

On the basis of this, the authors conclude the following:

The fact that the results show the G/G_o–γ curve high on the graph and the h–γ curve low is in agreement with what could be expected from sandy soil. It is generally accepted that the G/G_o–γ curve is higher in clayey soil than in sandy soil, while the h–γ curve is lower. Comparing with other recommended curve while it can be said that there are some discrepancies, these differences may be considered to be attributable to differences in testing equipment used.

4-3 Factors Influencing G/G_o–γ and h–γ Curves

While factors influencing G and h include void ratio, confining pressure, duration of

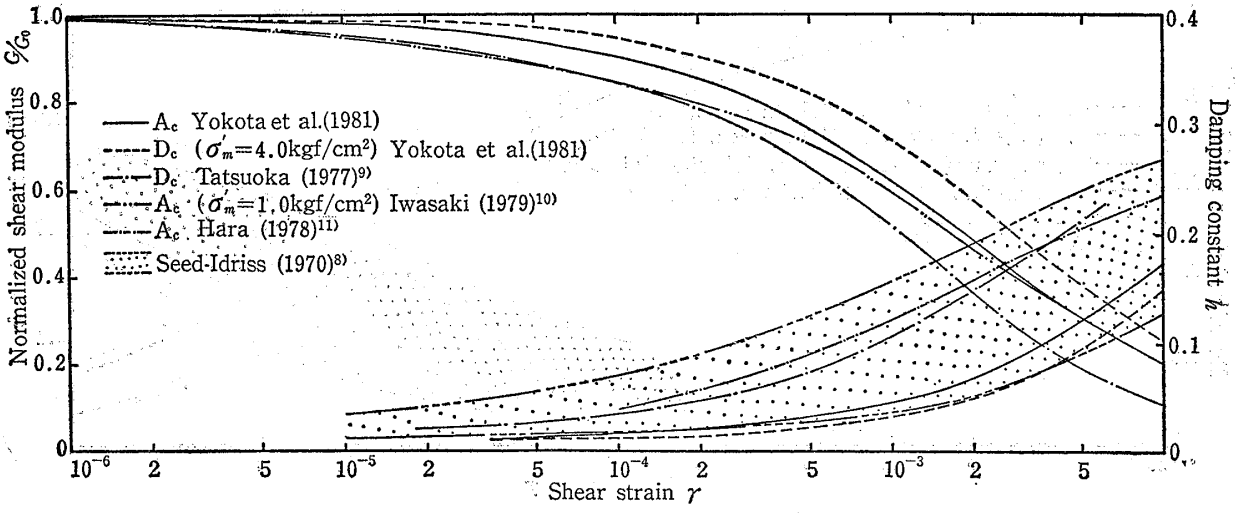

Fig. 23 Comparison with previously proposed curves of clayey soil

of consolidation, *OCR*, static shear strength, etc., our purpose here is to find the overall relationships between G/G_o–γ and h–γ, our tests have not been directed towards an analysis of these factors. The effect of these various factors on G are known. Unquestionably, these various factors have an effect on the G/G_o–γ and h–γ relationships. In particular, the problem of long term consolidation requires careful research.

4-4 Adequacy of Obtained G_o Values

Figure 24 is a comparison between G values obtained by in situ PS logging (G_{PS}) and G values when $\gamma=10^{-6}$, obtained by resonant column soil testing (G_{RC}). Because with G values obtained by PS logging as well, $\gamma \fallingdotseq 10^{-6}$, this comparison is important. By looking at the figure, we can see that generally $G_{PS} \geqq G_{RC}$. In Figure 25, this relationship is explored in more detail. From the figure, we may state the following:

(a) In both alluvial sandy soil and alluvial clayey soil, it holds that $G_{PS} \fallingdotseq G_{RC}$.

(b) We may say that in diluvial soil $G_{PS} \geqq G_{RC}$.

However, the authors' testing was carried out with isotropic consolidation pressure equal to effective overburden pressure. Thus, where average principal stress was used, it could not be expected that $G_{PS} \fallingdotseq G_{RC}$ for all alluvial soils.

Among the possible factors behind the relationship $G_{PS} \geqq G_{RC}$ in diluvial soil are:

(a) The degree of disturbance of the samples is considerably greater than that for alluvial soil.

(b) Because K_o is large for diluvial soils, in the tests, if adequate confining pressure is not applied, conditions approximating those for alluvial soil will not be satisfied.

In previous studies[5] as well as in the authors' study, we find that $G_{PS} \geqq G_{RC}$ for diluvial soil. However, in any case, judging from the relationships found in alluvial soil, we may conclude that our G_o values are valid.

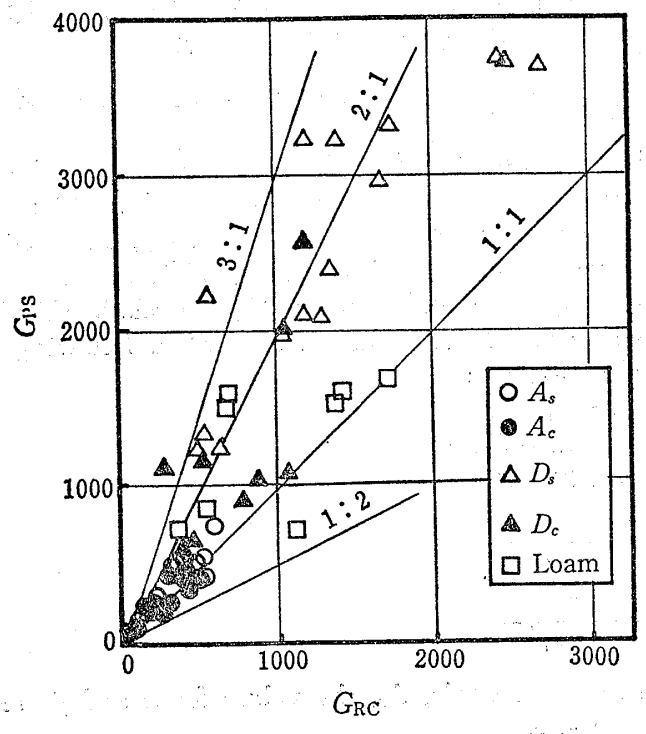

Fig. 24 Relationships between G_{PS} and G_{RC}

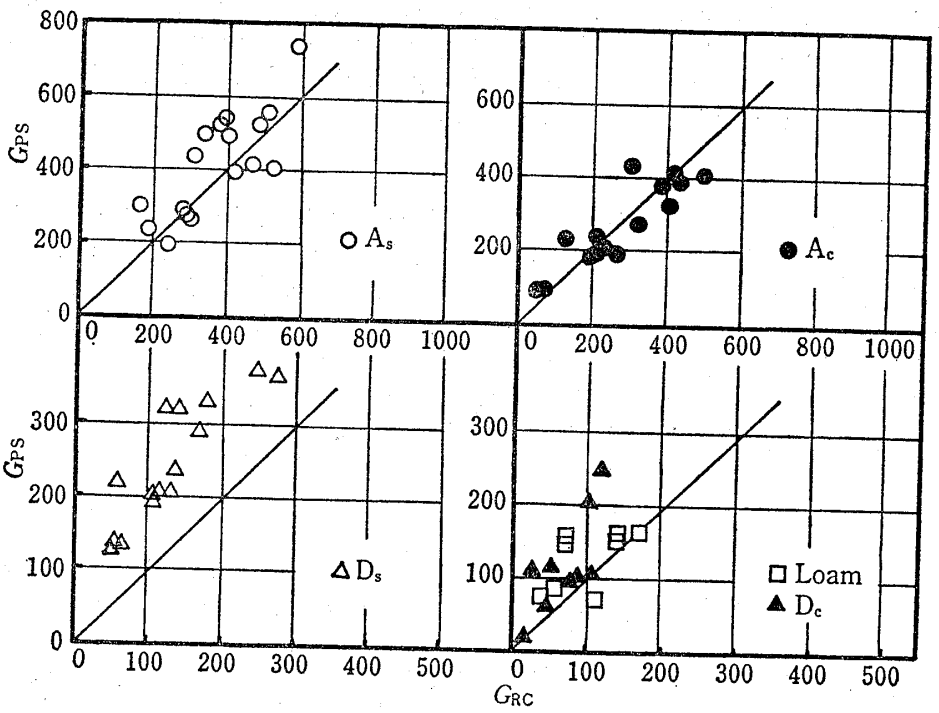

Fig. 25 Relationships between G_{PS} and G_{RC} (selected data)

5 SIMPLIFIED METHOD FOR EVALUATION OF DYNAMIC DEFORMATION CHARACTERISTICS OF SOIL

Here we will use the formulas cited above to propose a method for evaluating dynamic deformation characteristics of soil.

Figure 26 explains the procedure by which G and h may be easily determined by knowing N value, effective overburden pressure and shear strain. The basic thinking behind Figure 26 is as follows : Concerning the dependency of G on γ, the recommended curves that have been settled on after some debate and G when $\gamma \fallingdotseq 10^{-6}$ is taken as the value obtained by in-situ PS logging (i.e. $G=G_{PS}$), are used. In Figure 27, the relationship between N value and G_{PS} is shown[12]. Below is an example of an actual calculation following the procedure outlined in Figure 26. Conditions are as follows:

Soil type: A_s
σ'_v : 1.2kgf/cm²
γ : 3×10^{-3}
N value : 15

(1) Calculation of G/G_o

$$\frac{G}{G_o}=\frac{1}{1+\alpha\gamma^{\beta}} \tag{22}$$

For the soil type in the example, A_s, the values for α and β are as follows:

$$\left.\begin{aligned}\alpha&=120\times\sigma'^{-0.89}_{v}\\ \beta&=0.71\end{aligned}\right\} \tag{23}$$

Also, because $\sigma_v=1.2\text{kgf/cm}^2$,

$$\alpha=120\times1.2^{-0.89}$$

$$\beta=102$$

Also, because $\gamma=3\times10^{-3}$,

$$\frac{G}{G_o}=\frac{1}{1+102\times(3\times10^{-3})^{0.71}}$$

$$=0.377$$

(2) Calculation of G_{PS}

For soil type A_s, G_{PS} is calculated as follows:

$$G_{PS}=94.0\times N^{0.715} \tag{24}$$

If we substitute in $N=15$, we get

$$G_{PS}=44.0\times15^{0.715}$$

$$=652\text{kgf/cm}^2$$

(3) Calculation of G

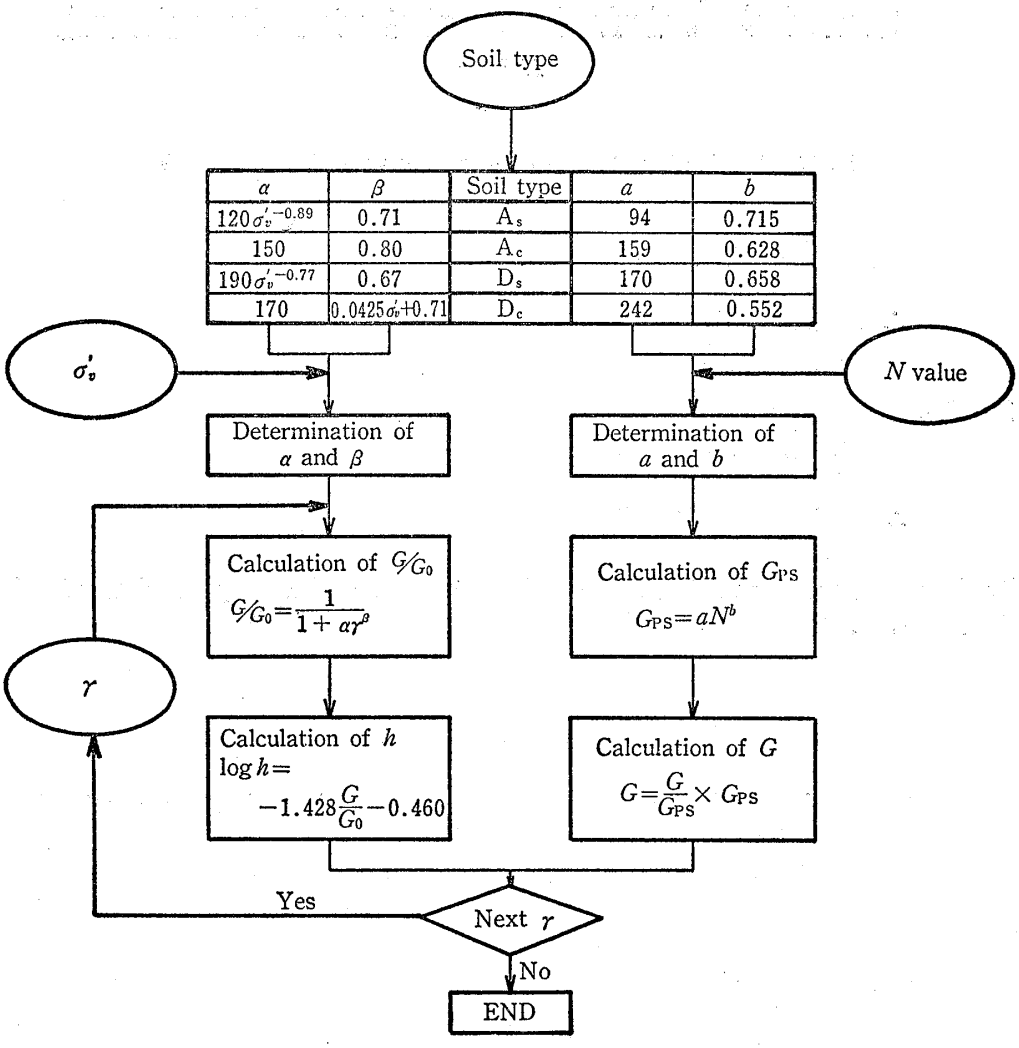

Fig. 26 Simple method of eveluating G and h for optional value of γ

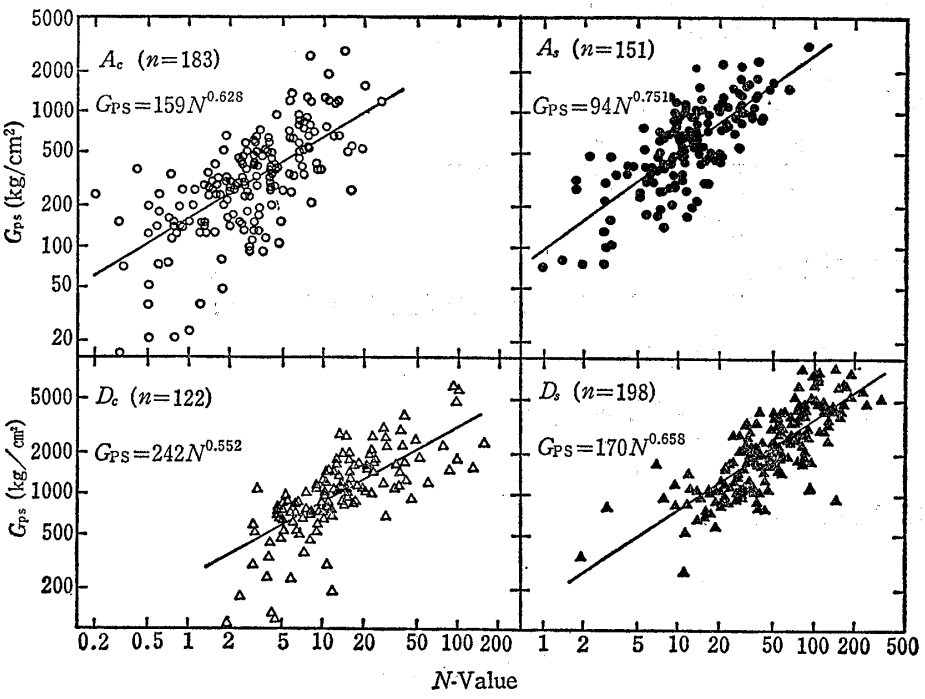

Fig. 27 Relationships between G_{PS} and N value (selected data)

$$G=\frac{G}{G_{PS}}\times G_{PS} \tag{25}$$

$$\therefore G=0.377\times 652$$
$$=246\text{kgf/cm}^2$$

(4) Calculation of h

$$h=10^{(-1.428\times G/G_o-0.460)} \tag{26}$$

$$\therefore h=10^{(-1.428\times 0.377-0.460)}$$
$$=0.100$$

By following the above method of calculation, G and h may be determined according to the conditions given.

6 CONCLUSION

Our study has shown that by using a simple set of formulas, the relationships G/G_o—γ and h-γ for the different soil types may be expressed. Heretofore, we have been forced to rely on average curves taken from a broad range. Frequently, these average curves were useless when a high degree of accuracy was called for. However, the present proposed curves are presented classified according to soil type, and thus may be said to have a much better level of accuracy. On the other hand, it must also be pointed out that other influencing factors have not been taken into account in the present study. Thus, the proposed formulas are no more than practical suggestions derived from the sphere of experience. Nevertheless, the authors' proposed simple quantitative method is highly effective in the evaluation of input data on ground response analysis during eathquakes.

As mentioned in this paper, a very important matter for future research is differences in test results due to differences in testing apparatus. For any proposed stress-strain relationship, the resulting model is necessarily based on the experimental results obtained by the researcher. However, dynamic testing is unlike the field of static testing in that the calibration of dynamic testing apparatus is extremely difficult. This is mainly attributable to the following factors:

(a) The inertia of the moving parts of the apparatus often results in complications.

(b) Very frequently error arises from minute friction.

(c) Occasionally significant influence is exerted by contact with such detection instruments as displacement transducers, etc.

(d) There are few methods for confirming whether or not obtained values are correct.

We may imagine that each of these factors combines together in different instruments in different ways, resulting in some incompatibility of results. At present, testing with Toyoura sand serves as a kind of calibrator. However, even in this case, it appears that results differ according to testing conditions, method of preparation of specimens, density measurement, etc. Probably the time has come to consider creation of unified testing standards for each type of test apparatus.

As we can expect that there will be more and more of a demand for accurate analysis techniques, the development of improved testing apparatus and methods may be regarded as extremely important.

References

1) B. O. Hardin and V. P. Drnevich (1972): "Shear Modulus and Damping in Soils; Design Equations and Curves" Journal of the Soil Mechanics and Foundations Division, ASCE, Vol. 98, SM 7, pp. 667–692.

2) K. Zen, Y. Umehara and K. Hamada (1978): "Laboratory Tests and In-Situ Seismic Survey on Vibratory Shear Modulus of Clayey Soils with Various Plasticities", Proc. 5th Japanese Earthquake Engineering Symposium-1978, pp. 721–728.

3) T. Iwasaki, K. Tokida and S. Yosida (1979): "Dynamic Deformation Characteristics in Alluvial Clayey Soils —Strain-Dependence of Shear Moduli—" (in Japanese), Bulletin of Public Works Research Institute, Ministry of Construction No. 1504, pp. 83–84.

4) T. Kokusho, A. Sakurai and Y. Esashi (1978): "Development of a Dynamic Soil Testing Method Using A Triaxial Cell for Very Small to Large Strain and Application to Testing on Properties of Sands" (in Japanese), Proc. 14th Annual Meeting JSSMFE, pp. 537–540.

5) T. Kokusho, M. Sasaki (1979): "Determination of Dynamic Soil Properties of Undisturbed Diluvial Sand Deposit Samples by Cyclic Triaxial Testing" (in Japanese), Proc. 15th Annua Meeting JSSMFE, pp. 537–540.

6) Y. Takagi, F. Tatsuoka and S. Yoshida (1972): "Shear Moduli and Damping Constant of Sand under Torsional Loading of Hollow Cylindrical Specimens" (in Japanese), Proc. 32th Annual Meeting JSCE, pp. 263–264.

7) F. Tatsuoka and Y. Takagi (1977): "Strain-Dependence of Shear Modulus and Damping in Sands" (in Japanese), Proc. 12th Annual Meeting JSSMFE, pp. 417–420.

8) "Dynamic Interaction between Soil and Structure" (in Japanese), (1973) Publication of JSSMFE, pp. 39–42.

9) T. Iwasaki, F. Tatsuoka and K. Yokota (1977): "Results of Laboratory Test for Shear Modulus on Undisturbed Clay" (in Japanese), Proc. 12th Annual Meeting JSSMFE, pp. 433–436.

10) T. Iwasaki, F. Tatsuoka and S. Yoshida (1978): "Dynamic Deformation Characteristics of Alluvial Clayey Soils As Determined By Resonant-Column Test and Triaxial Testing" (in Japanese), Proc. 13th Annual Meeting JSSMFE, pp. 569-572.
11) Y. Ohsaki, A. Hara and K. Yoshihara (1978): "Stress-Strain Model of Soils for Seismic Analysis", Proc. 5th Japan Earthquake Engineering Symposium-1978, pp. 697-700.
12) T. Imai (1977): "P-and S-Wave Velocities of the Ground in Japan", Proc. 9th ICSMFE, Vol. 2, pp. 257-260.

室内動的土質試験から得られた土の動的変形特性

横田耕一郎・今井常雄・今野政志

概　要

土の動的変形特性 (dynamic deformation characteristics) を知ることは，地震時の地盤の挙動 (behavior of the ground) を予測するうえで極めて重要である。筆者等は，この土の動的変形特性を調べるために，数多くの室内土質試験 (laboratory soil tests) を実施し，動的変形特性の一般的表現を求め，実用的簡易評価法の検討を行なった。その結果をとりまとめて報告する。

今回調べた特性は，具体的には，土のせん断弾性係数 (shear modulus) G，および減衰定数 (damping constant) h と，せん断歪 (shear strain) γ との関係である。G, h, および γ を求めるために用いた試験機 (testing apparatus) は，共振法土質試験機 (resonant column soil test apparatus)，繰り返しねじり試験機 (cyclic torsional test apparatus) の2種類である。共振法土質試験は，三軸セル (triaxial cell) 内に設置された下端固定の供試体 (specimen) にねじり振動 (torsional vibration) を与え，その時の共振振動数 (resonant frequency) から，試料の硬さ，すなわち，G を算定すると共に，共振時 (resonant state) の供試体回転速度 (rotational velocity of the specimen) から γ を求めるものである。この試験は，$10^{-6}<\gamma\leqq10^{-4}$ 程度の範囲での G を求めることができる。繰り返しねじり試験は，同じく，下端固定の供試体に対し，上端にねじり力を与え，その時の回転角 (rotational angle) とトルクを測定することにより，G, h, γ の関係を求めるものである。この試験は，$10^{-4}<\gamma\leqq10^{-2}$ 程度の範囲での G, h を求めるのに適している。図—1および図—2には，それぞれ共振法土質試験，繰り返しねじり試験の原理を，また，図—3は繰り返しねじり試験より h を求める方法を示す。図—4には，両試験機の試験装置を，図—5(a)および(b)には測定系統を示してある。

表—1は，今回試験に用いた全試料のリストであり，試料数は全部で79試料である。表—2は，主な試験条件を示したものである。

図—6および図—7には，このようにして測定した結果の1例を示す。図—6は G と γ の関係，図—7は $h\sim\gamma$ の関係の例である。

図—8および図—9は今回の実験結果のすべてを図示したものである。ただし，G は G を G_0（$\gamma=10^{-6}$ での G）で除して標準化してある。かなり広い範囲にばらついていることがわかる。

図—10～図—13は，土の種類毎に分けて示した $G/G_0\sim\gamma$ および $h\sim\gamma$ の関係である。砂質土 (sandy soil) と粘性土 (clayey soil) で明瞭な違いのあることがよくわかる。Hardin and Drnevich[1] によれば，G/G_{max} はつぎのように示すことができる。

$$\frac{G}{G_{max}}=\frac{1}{1+\dfrac{\gamma}{\gamma_r}} \qquad (1)$$

ただし，G_{max}：G の最大値 ($\fallingdotseq G_0$)
γ_r：規準歪 (reference strain)
($\gamma_r=\dfrac{\tau_{max}}{G_0}$, τ_{max}：せん断強度)

γ_r は一つの試料については一定のはずであるが，(1)式から，実験時の G/G_0 と γ の組に対して逆算した γ_r は，異なる γ に対して一定の値をとらない。そこで，$\gamma_r=A(\gamma)$ とおき，(1)式から逆算して $A(\gamma)$ と γ の関係を

示したものが図—14である。log $A(\gamma)$ と log γ は直線関係にあることがわかる。この関係を用いて(1)式を書き換えると，(1)式は

$$\frac{G}{G_0}=\frac{1}{1+\alpha\gamma^{\beta}} \tag{2}$$

となる。ただし，α および β は log $A(\gamma)$ と log γ の切片と傾きに関係する係数である。

図—15～図—17は，α および β と有効上載圧 (effective overburden pressure) σ'_v および塑性指数 (plasticity index) I_p との関係を調べたものである。表—3にこれらの関係から判明した α および β の最適値 (optimum value) を，σ'_v の関数，あるいは平均値 (average value) として示した。

図—18は，h と G/G_0 との関係を調べたものである。図には，データの分布している範囲の，ほぼ平均的と思われる曲線と，この曲線を表わす式を示してある。表—3と，この曲線を表わす式を用いれば，各種の土に対して $G/G_0\sim\gamma$ と $h\sim\gamma$ の標準曲線(recommended curve)を定めることができる。図—19～図—21に，これらの標準曲線を示す。

図—22および図—23は，それぞれ砂質土および粘性土に関して，今回定めた標準曲線と既存の発表されている標準曲線を比較したものである。今回のデータは，全般には，既存データと比べて $G/G_0\sim\gamma$ ではやや上方に，$h\sim\gamma$ ではやや下方に位置している。細かくみると，洪積砂質土 (diluvial sandy soil) のように非常に良く合っている既存データもあり，また，相当異っているものもある。

これらの差異は，主として，それぞれの機関で用いている試験装置のうち，セルの構造，とくにピストン部の構造の違い，さらに，応力および変位の検出システムの違いによるものと考えられる。現状においては，いずれの結果を妥当な値としてよいか，一概にいえない。

図—24および図—25は，原位置PS検層 (in-situ PS logging) で求めた $G(=G_{PS})$ と，共振法土質試験で求めた $G(=G_{RC})$ との比較を示したものであり，今回求めた G_{RC} の妥当性を検討するために示した図である。これを見ると，沖積土では，大体，$G_{PS}\fallingdotseq G_{RC}$ が成り立つ。また，洪積土では $G_{PS}\geqq G_{RC}$ であるが，他の研究機関の結果でも，一般的に $G_{PS}\geqq G_R$ (G_R：室内試験での $\gamma\fallingdotseq10^{-6}$ における G) の傾向となっており，今回の実験結果の G_{RC} のレベルは妥当なものと考えられる。

以上の検討結果をもとに，任意の土質，N値，有効上載圧，が与えられた時の $G\sim\gamma$，$h\sim\gamma$ の関係を直ちに求め得る実用的な簡易評価法を提案した。図—26が，その手順である。これは地震時の地盤応答解析 (response analysis of the ground)において，地盤物性に関する入力値の評価に大変有効である。